Positron-hydrogen scattering at low intermediate energies

M. Z. M. Kamali[1] and Kuru Ratnavelu[1,2]

[1]*Quantum Scattering Theory Group, Institute of Mathematical Sciences, University of Malaya, 50603 Kuala Lumpur, Malaysia*
[2]*Department of Physics and Astronomy, University of Oklahoma, Norman, Oklahoma 73069*
(Received 20 June 2001; published 11 December 2001)

We apply the coupled-channel-optical method for positron-hydrogen atom scattering at energies just above the ionization threshold to 40 eV. The rearrangement positronium channels are treated in the close-coupling method that includes the atomic target states. The neglect of the continuum is taken into account via an *ab initio* optical potential model. Physical observables such as ionization, positronium formation, and total cross sections are presented together with elastic and positronium($1s$) differential cross sections.

Its undeniable that experimental developments in the field of positron-hydrogen atom scattering had made major strides in the 1990s [1–5]. Most of these experimental measurements had reported total, positronium (Ps) formation and ionization cross sections from low to high energies. As far as we are aware, there are no differential cross section (DCS) measurements done yet on the positron-H system. Although we have seen much work on the low-energy region [6–8], there has been a lack of theoretical studies for positron-hydrogen atom system, especially, in the intermediate and high energies (see Rajagopal and Ratnavelu [9] for a discussion on other theoretical works). Recently, we have seen further work by Kar and Mandal [10] and Janev and Solovev [11] that have added newer results for positron-H scattering at intermediate energies. Kar and Mandal have comprehensively studied the Ps($1s$) DCS for a large range of intermediate energies using the Schwinger variational method. They found very interesting features in the DCS that has motivated our present report. The advanced adiabatic work (also sometimes called as ''hidden-crossing theory'') of Janev and Solovev has also shown fair agreement with available experimental and theoretical methods for Ps formation and ionization cross sections.

The present paper extends the work of Rajagopal and Ratnavelu [9] and will concentrate on the lower intermediate energies that range just above the ionization threshold to about 40 eV. We will also report total cross sections, ionization cross sections, and Ps formation cross sections and also elastic and Ps($1s$) DCS and compare where, available with experimental and other theoretical data.

The theoretical details of the coupled-channels optical method (CCOM) had been presented in the work of Rajagopal and Ratnavelu [9] and the full formalism of the close-coupling (CC) method can be found in Refs. [12,13]. Essentially, the Schrödinger equation for the positron-hydrogen atom system can be transformed to a set of coupled momentum-space Lippmann-Schwinger equations for a positron with the momentum k incident on a hydrogen atom in state Ψ_α (atomic units are used throughout) are

$$
\begin{aligned}
&\langle \mathbf{k}'\Psi_{\alpha'}|T|\mathbf{k}\Psi_\alpha\rangle \\
&= \langle \mathbf{k}'\Psi_{\alpha'}|V^Q|\mathbf{k}\Psi_\alpha\rangle \\
&\quad + \sum_{\alpha''}\int d^3k'' \frac{\langle \mathbf{k}'\Psi_{\alpha'}|V^Q|\mathbf{k}''\Psi_{\alpha''}\rangle\langle \mathbf{k}''\Psi_{\alpha''}|T|\mathbf{k}\Psi_\alpha\rangle}{\left(E^{(+)}-\varepsilon_{\alpha''}-\frac{1}{2}k''^2\right)} \\
&\quad + \sum_{\beta''}\int d^3k'' \frac{\langle \mathbf{k}'\Psi_{\alpha'}|V|\mathbf{k}''\Phi_{\beta''}\rangle\langle \mathbf{k}''\Phi_{\beta''}|T|\mathbf{k}\Psi_\alpha\rangle}{\left(E^{(+)}-\varepsilon_{\beta''}-\frac{1}{4}k''^2\right)} \quad (1)
\end{aligned}
$$

$$
\begin{aligned}
&\langle \mathbf{k}'\Phi_{\beta'}|T|\mathbf{k}\Psi_\alpha\rangle \\
&= \langle \mathbf{k}'\Phi_{\beta'}|V|\mathbf{k}\Psi_\alpha\rangle \\
&\quad + \sum_{\alpha''}\int d^3k'' \frac{\langle \mathbf{k}'\Phi_{\beta'}|V|\mathbf{k}''\Psi_{\alpha''}\rangle\langle \mathbf{k}''\Psi_{\alpha''}|T|\mathbf{k}\Psi_\alpha\rangle}{\left(E^{(+)}-\varepsilon_{\alpha''}-\frac{1}{2}k''^2\right)} \\
&\quad + \sum_{\beta''}\int d^3k'' \frac{\langle \mathbf{k}'\Phi_{\beta'}|V|\mathbf{k}''\Phi_{\beta''}\rangle\langle \mathbf{k}''\Phi_{\beta''}|T|\mathbf{k}\Psi_\alpha\rangle}{\left(E^{(+)}-\varepsilon_{\beta''}-\frac{1}{4}k''^2\right)}.
\end{aligned}
$$

$$(2)$$

In the above equations, Ψ_α and Φ_β are the hydrogen and positronium states, respectively. The generic term V is used to label the interaction between the different classes of channels and the details of the V^Q can be found in Ref. [9].

The following calculations were performed in the present work:

CC(3,3): The $n=1$ and 2 hydrogen ($1s$, $2s$, and $2p$), states are included in the close-coupling expansion together with the Ps($1s$), Ps($2s$), and Ps($2p$) states.

CCO(3,3): The continuum potentials for the $1s$-$1s$, $1s$-$2s$, $1s$-$2p$, $2s$-$2s$, $2s$-$2p$, and $2p$-$2p$ are used within the CC(3,3). At energies below 30 eV, only the $1s$-$1s$, $1s$-$2s$, and $1s$-$2p$ continuum channels were used.

CC(6,3): Here the $n=1,2$ and 3 ($1s$, $2s$, $2p$, $3s$, $3p$, and $3d$) hydrogen states are included in the expansion together with the three physical Ps ($1s$, $2s$, and $2p$) states.
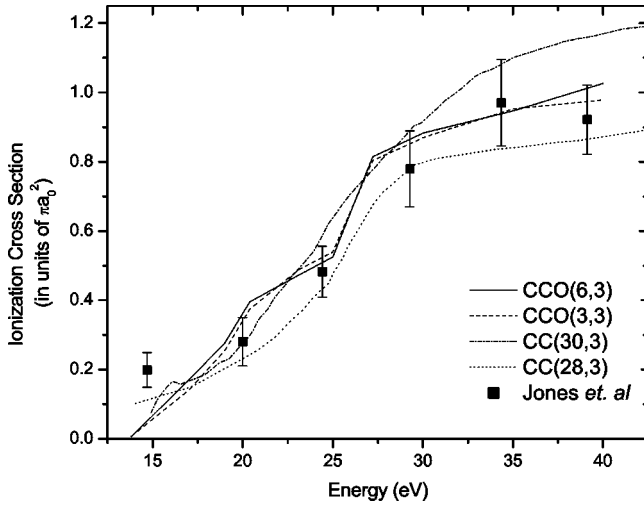
FIG. 1. Ionization cross sections for positron-hydrogen atom scattering. Theoretical data: CCO(6,3) (solid), CCO(3,3) (dash), CC($\overline{28}$,3) (dot), and CC($\overline{30}$,3) (dash-dot); experimental data: Jones *et al.* (squares).

CCO(6,3): The continuum potentials for the $1s$-$1s$, $1s$-$2s$, $1s$-$2p$, $2s$-$2s$, $2s$-$2p$, and $2p$-$2p$ are used within the CC(6,3). At energies below 30 eV, only the $1s$-$1s$, $1s$-$2s$, and $1s$-$2p$ continuum channels were used.

The similarity of the nomenclature between the CCO(m,n) and CC(m,n) is due to the fact that in both cases the total wave function for the system is expanded in the close-coupling basis [13] and in the CCO(m,n) case, the continuum optical potentials are explictly included in the V^Q [see right-hand side of Eq. (1)].

We follow the procedure of Ratnavelu, Mitroy, and Stelbovics [14] by implementing a five-panel composite mesh so that sufficient grid density is generated near both the e^+-H and Ps-p on-shell momenta. We have obtained converged results using 56–68 quadrature points for all energies. The Ps formation rearrangement terms [see Eq. (35) of [13]] are included up to $J=22$ for all energies studied. In the CCO calculations, the optical potentials were included to a maximum $J=J_{opt}$ (where $J_{opt}=24$ at 40 eV). These are supplemented with the CC(6,3) partial-wave T matrices until $J=J_{max}$ (at 40 eV, $J_{max}=36$).

In Fig. 1, we display the present calculations CCO(6,3) and CCO(3,3) for the ionization cross sections (ICS). We also show the CC($\overline{28}$,3) calculations of Mitroy [7] and the CC($\overline{30}$,3) calculations of Kernoghan *et al.* [8]. The experimental measurements [3] are also shown. Our present ICS supercedes the earlier reported work [9,11] at 30 eV and 40 eV. This has been due to improvements in the numerical aspects of the calculations. Nevertheless, the differences are minor. Our present data show similar qualitative trends as the experimental measurements of Jones *et al.* [3] and the theoretical works of Mitroy [7] and Kernoghan *et al.* [8]. There are some differences in detail for $E < 27$ eV between the present work and the other theoretical data. Considering these differences in treating the continuum by the various theoretical methods, it is quite evident that the qualitative and to some extent the quantitative features of the ionization
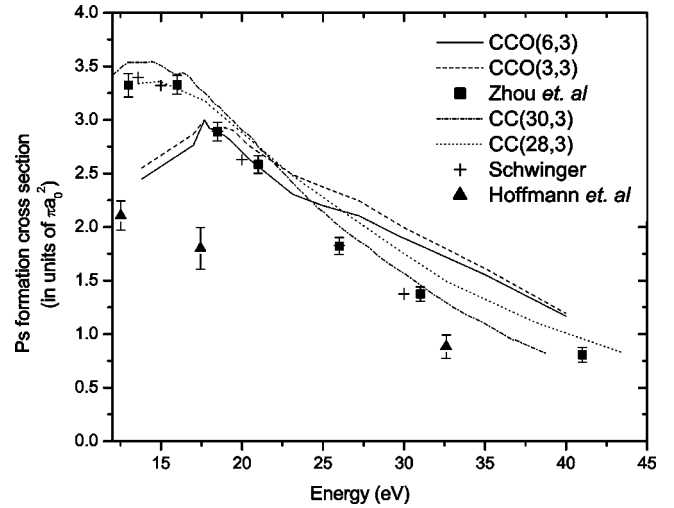

FIG. 2. Total positronium formation cross sections for positron-hydrogen atom scattering. Theoretical data: CCO(6,3) (solid), CCO(3,3) (dash), CC($\overline{28}$,3) (dot), CC($\overline{30}$,3) (dash-dot), and Schwinger Model (+): experimental data: Zhou *et al.* (squares) and Hoffmann *et al.* (triangles).

cross sections for positron-hydrogen scattering in this energy regime is being described quite well.

In Fig. 2, we show the CCO(6,3) and CCO(3,3) total Ps cross sections with the CC($\overline{28}$,3), CC($\overline{30}$,3) and the Schwinger calculation of Kar and Mandal [10] (we will term it as the Schwinger model). The experimental measurements of Zhou *et al.* [2] and Hoffmann *et al.* [5] are also shown. Although all theoretical models show the general trend, there are nevertheless differences. The two experimental measurements also show vast differences below 20 eV. The Schwinger model only gives the Ps($1s$) cross section and is shown here for comparative purposes. In comparing the Schwinger model with the close-coupling models suggest that the contribution of the higher Ps($n=2$) states to the total Ps formation cross sections are still significant for energies below 40 eV. The differences between the CCO models and the larger CC($\overline{28}$,3) is within 5–10 % for $E>20$ eV. Below 20 eV, there is a dramatic drop between the present models and other works. This difference could mainly be due to the smaller P space used in the CCO calculations as the present CC(6,3) shows the same trend. We note that the present data below 17 eV seems to be closer to the data of Hoffmann. The excellent agreement between the Schwinger-model cross sections [which excludes the Ps($2s$) and Ps($2p$)] at all energies with Zhou's total Ps cross sections will disappear if they include Ps($2s$) and Ps($2p$) cross sections. Thus, it would be interesting to see further work for an accurate study of the Ps cross sections at these lower intermediate energies. To provide an idea of the quality of the present work, we can compare the Ps($1s$) of the CCO(6,3) with the Schwinger model. At about 13.8 eV the CCO(6,3) gives a Ps($1s$) cross section of $2.38\pi a_0^2$ (while Schwinger model's at 13.6 eV is $3.399\pi a_0^2$). At 30 eV, the CCO(6,3) cross section is $1.477\pi a_0^2$ and the Schwinger model is $1.374\pi a_0^2$. At 40 eV, we find the differences become smaller (CCO(6,3): 0.819 πa_0^2 and Schwinger: $0.7758\pi a_0^2$). This provides ample jus-
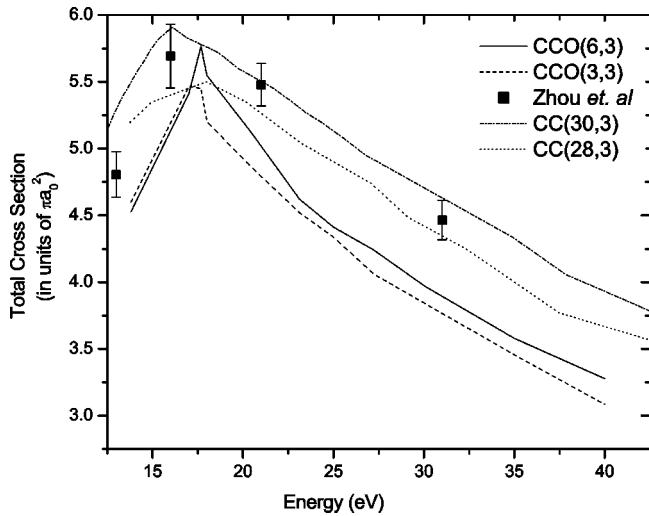
FIG. 3. Total cross sections for positron-hydrogen atom scattering. Theoretical data; CCO(6,3) (solid), CCO(3,3) (dash), CC($\overline{28}$,3) (dot), and CC($\overline{30}$,3) (dash-dot); experimental data: Zhou *et al.* (squares).

tification that the CCO calculations are quite reliable for E >20 eV.

The calculated total cross sections (TCS) are shown in Fig. 3, in general, the optical potential enhances the cross sections. The dramatic effect is seen at around the peak of the TCS and just above the ionization threshold. Here, the CCO(6,3) and the CCO(3,3) enhances the TCS by about $30-40\%$. The sharp peak in the TCS at around the $17-18$ eV region is plausibly due to the insufficient P space used in the present calculations. At other energies, the effects of the continuum is less spectacular but still very significant. This suggests that the CCO is probably modeling the continuum quite well at the energies just above the threshold. The closer agreement between experimental data of Zhou *et al.* and the larger L^2 models suggests that the present CCO calculations should show better TCS with a larger P space.

Our CCO(6,3) DCS for the Ps($1s$) are shown with the Schwinger calculations at 13.8, 20, 30, and 40 eV in Figs. 4(a) and 4(b). We have chosen not to depict the CCO(3,3) as it will clutter the figures. Essentially, there are some differences in magnitude between the CCO(6,3) and CCO(3,3) but
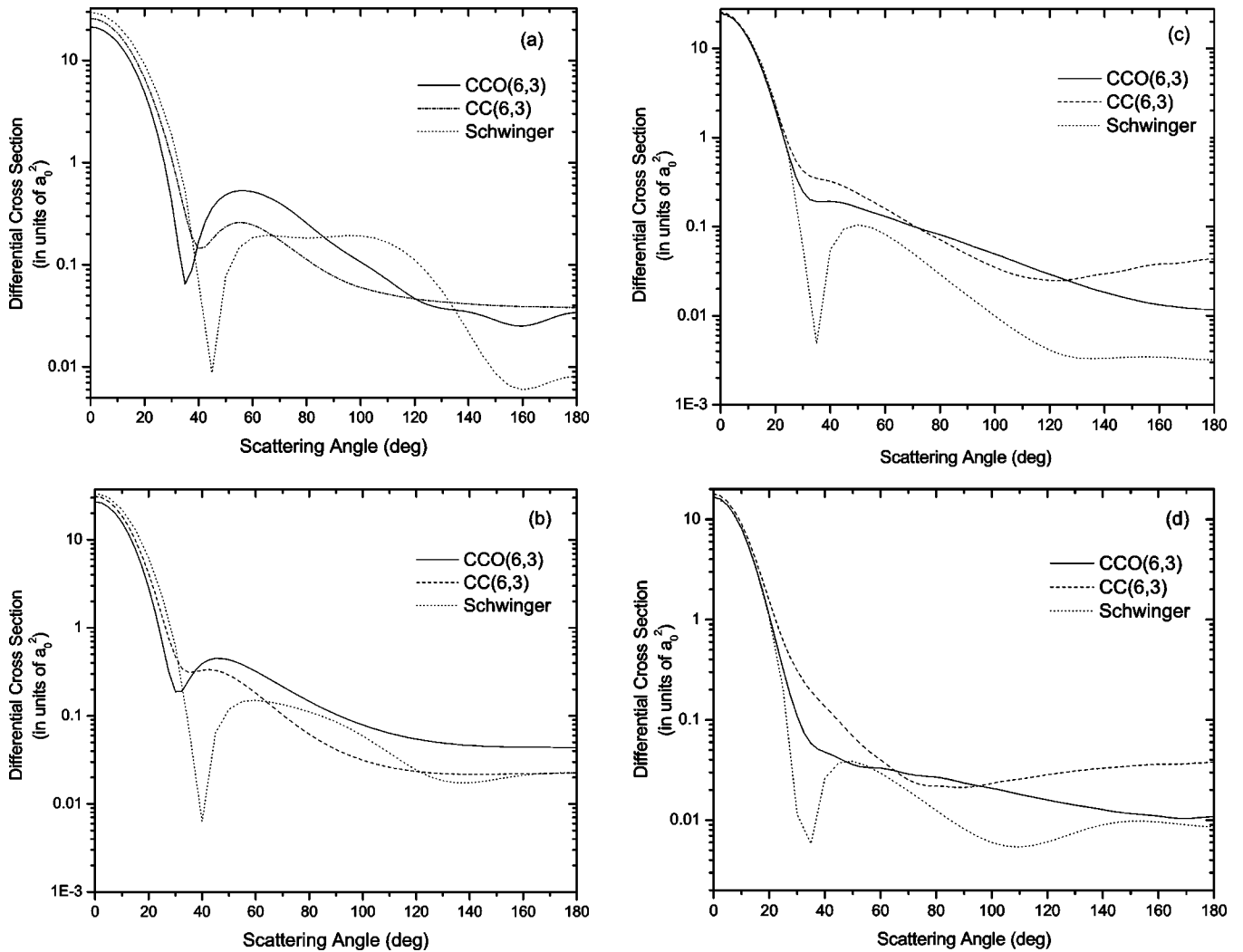

FIG. 4. Ps($1s$) differential cross sections for positron-hydrogen atom scattering at (a) 13.82 eV, (b) 20.41 eV, (c) 30 eV, and (d) 40 eV. Theoretical data: CCO(6,3) (solid), CC(6,3) (dash), and Schwinger model (dot).
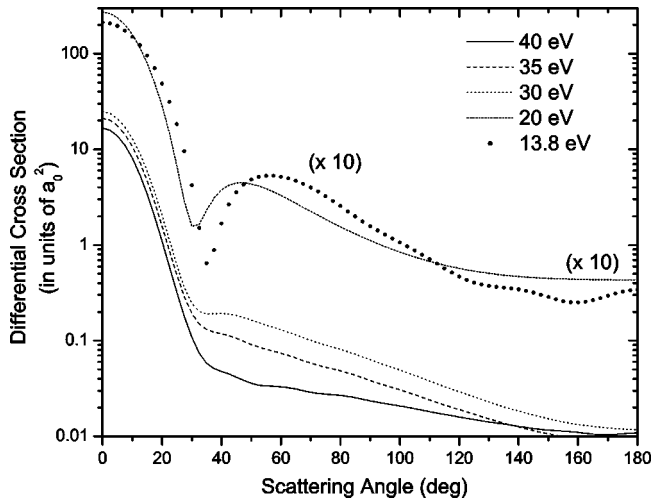
FIG. 5. Ps DCS for positron-hydrogen atom scattering at various energies using the CCO(6,3).

FIG. 6. Elastic DCS for positron-hydrogen atom scattering at various energies using the CCO(6,3).

the same trends are observed. In general, we find the first minima predicted by Kar and Mandal is also present at all these energies but the depth of this minima becomes shallower as the incident energy increases. The interesting aspect of the DCS given by Kar and Mandal is that the first minima is very prominent even at 40 eV as it was at 13.6 eV. The second minima at the backward angles as predicted by the Schwinger model is not clearly observable by our models except at 13.8 eV. To further illustrate the trend of the our DCS, we exhibit the CCO(6,3) DCS only in Fig. 5. For purposes of clarity, the DCS at 13.8 eV and 20 eV have been magnified ten times. As we go from 13.8 eV to 20 eV, we find the forward minima becomes shallower and the position of the minima moving to small angles. At 30 eV, this is still evident with a wider but very shallow minima. At 35 and 40 eV, there exists a shoulder in the region between $30°$–$40°$.

For completeness, we also show the CCO(6,3) elastic DCS at 13.8 eV, 20 eV, 30 eV, and 40 eV in Fig. 6. We clearly observe a deep and wide minima at about $50°$ for the 13.8 eV case. At 20 eV, we only observe a shallow trough and for 40 eV, we see no trace of this minima.

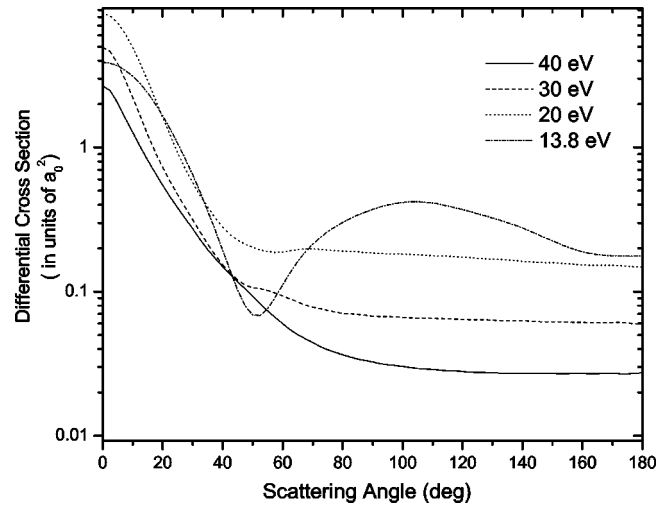In conclusion, we have performed a series of coupled-channels-optical calculations for positron-hydrogen scatter-ing at low intermediate energies ranging from just above the threshold to 40 eV. The larger L^2 models and the present CCO models treat the continuum differently. The L^2 uses pseudostate orbitals in the target expansion and the CCO uses an *ab initio* optical potential for the continuum. Thus, the close agreement between theory and experiment for the ICS suggests that both methods are doing quite well. The largest disparity between the present calculations and the other theoretical data at $E<20$ eV for the total Ps cross sections is very glaring. The present results for the total cross sections also suggest that a larger P space CCO calculation would be needed.The differential cross sections calculated for the Ps($1s$) formation is highly interesting as is the elastic DCS.

[1] G. Laricchia and M. Charlton, in *Positron Beams and its Applications*, edited by P. G. Coleman (World Scientific, Singapore, 2000), p. 41.

[2] S. Zhou, H. Li, W.E. Kauppilla, C.K. Kwan, and T.S. Stein, Phys. Rev. A **55**, 361 (1997).

[3] G.O. Jones, M. Charlton, J. Slevin, G. Laricchia, A. Kover, M.R. Poulsen, and S.N. Chromaic, J. Phys. B **26**, L483 (1993).

[4] M. Weber, A. Hoffmann, W. Sperber, F.M. Jacobsen, and K.G. Lynn, Hyperfine Interact. **89**, 221 (1994).

[5] A. Hoffmann, T. Falke, W. Raith, M. Weber, D.P. Becker, and K.G. Lynn, J. Phys. B **30**, 3297 (1997).

[6] J.W. Humberston, J. Phys. B **17**, 2353 (1984).

[7] J. Mitroy, Aust. J. Phys. **50**, 751 (1996).

[8] A.A. Kernoghan, D.J.R. Robinson, M.T. McAlinden, and H.R.J. Walters, J. Phys. B **29**, 2089 (1996).

[9] K.K. Rajagopal and K. Ratnavelu, Phys. Rev. A **62**, 022717 (2000).

[10] S. Kar and P. Mandal, Phys. Rev. A **62**, 052514 (2000).

[11] R.K. Janev and E.A. Solovev, J. Phys. B **32**, 3215 (1999).

[12] K. Ratnavelu and K.K. Rajagopal, J. Phys. B **32**, L381 (1999).

[13] J. Mitroy, Aust. J. Phys. **46**, 751 (1993).

[14] K. Ratnavelu, J. Mitroy, and A.T. Stelbovics, J. Phys. B **29**, 2775 (1996).